Low pump limit of the bifurcation to periodic intensities in a semiconductor laser subject to external optical feedback

G. Lythe and T. Erneux
Université Libre de Bruxelles, Optique Nonlinéaire Théorique, Campus Plaine, Code Postal 231, 1050 Bruxelles, Belgium

A. Gavrielides and V. Kovanis
Nonlinear Optics Center, Phillips Laboratory PL/LIDN, 3350 Aberdeen Avenue SE, Kirtland Air Force Base, New Mexico 87117-5776

(Received 4 June 1996; revised manuscript received 15 October 1996)

The conditions for a bifurcation to periodic intensities (Hopf bifurcation) for low values of the pump current are examined using singular perturbation methods. We show that the frequency of the oscillations at the bifurcation point remains close to the relaxation oscillation frequency of the solitary laser until the pump parameter is close to its effective threshold value. This part of our analysis adds substance to previous estimates of the frequency of the oscillations, which were guided by experiments. In the second part of our analysis, we show that, very close to threshold, the frequency exhibits a sharp transition from the relaxation oscillation frequency to a frequency proportional to the external cavity frequency (i.e., $2\pi/\tau$, where τ is the external round-trip time). [S1050-2947(97)06805-4]

PACS number(s): 42.65.Sf, 42.60.Mi

I. INTRODUCTION

A semiconductor laser subject to weak optical feedback quickly exhibits chaotic intensity oscillations as the feedback rate is increased. A particular form of chaotic output called low-frequency intensity fluctuations (LFF) is observed when the laser operates close to its solitary threshold [1]. LFF's are characterized by successive dropouts of the average laser intensity, followed by slow recoveries. Recent numerical simulations have improved our understanding of the dynamical mechanisms responsible for LFF [2,3], but analytical information on the bifurcation possibilities remain rare due to the complexity of the laser equations.

Earlier investigations of LFF revealed that the LFF main frequency is much smaller than the relaxation oscillation (RO) frequency of the solitary laser, which dominates as the laser operates far above threshold. They suggested that the external cavity (EC) may have a stronger effect as the pump current is progressively decreased. Following this idea, Fujiwara, Kubato, and Lang [4] proposed a frequency of the form $f \sim f_{\mathrm{RO}}/\sqrt{\gamma\tau}$, where f_{RO} is defined as the RO frequency and γ and τ are the feedback rate and the delay time of the feedback, respectively. Later, Tatah and Garmire [5] and Sacher, Elsasser, and Gobel [6] derived a frequency of the form

$$f \sim f_{\mathrm{RO}}/\sqrt{1+\gamma\tau}. \tag{1}$$

The expression (1) is based on several simplifications of the characteristic equation, which describes the stability of a single frequency solution (constant intensity). For low values of the pump above threshold, intensity oscillations are expected to appear at higher feedback rates (higher γ), which then implies, according to Eq. (1), a frequency f lower than f_{RO}.

However, the small pump limit of the characteristic equation is a delicate limit, because it depends on how we compare the pump parameter to other small parameters in the problem. The main objective of this paper is to derive a systematic approximation of the Hopf bifurcation frequency and discuss its behavior as the pump parameter is progressively decreased.

In order to examine the small pump limit of the laser equations, it is necessary to formulate these equations in dimensionless form so that we may identify and relate different small or large parameters. In [7], two large parameters were related to find an approximation of the Hopf bifurcation point for arbitrary values of the pump parameter P. These large parameters are $T \equiv \tau_n \tau_p^{-1}$ and $\theta \equiv \tau \tau_p^{-1}$ where τ_n, τ_p, and τ denote the carrier lifetime, the photon lifetime, and the external round-trip time, respectively. Typical values of these time constants ($\tau_p \sim 2$ ps, $\tau_n \sim 2$ ns, and $\tau \sim 1-10$ ns) imply that $T \sim \theta \sim 10^3$. The advantage of an approximation of the Hopf bifurcation point based on the large values of T and θ is discussed in [8]. However, this approximation fails mathematically for low values of P, which suggests that a different limit may exist for a specific scaling between T, θ, and P. After relating these parameters, we derive new and richer equations for the Hopf bifurcation point, which we analyze in detail.

In Sec. II, we formulate the dimensionless Lang and Kobayashi equations. We then show that the frequency of the oscillations admits two different limits corresponding either to the RO frequency or to an EC frequency. Sections III and IV are the technical sections and lead to two separate approximations of the Hopf bifurcation point. Section V summarizes the main results in terms of the original parameters. Section VI examines the validity of the expression (1) and discusses the physical meanings of the RO and EC domains. All nonstandard mathematical details are described in the Appendix and are not essential for the comprehension of our main results.

II. FORMULATION

Lang and Kobayashi [9] have considered a laser diode exposed to optical feedback from a flat external mirror. For

weak to moderate feedback, the laser is modeled by the following dimensionless rate equations for the electrical field Y and the excess carrier number Z [7,10]:

$$\frac{dY}{ds}=(1+i\alpha)ZY+\eta\,\exp(-i\Omega_0\theta)Y(s-\theta), \tag{2}$$

$$T\frac{dZ}{ds}=P-Z-(1+2Z)|Y|^2. \tag{3}$$

In these equations, s is time measured in units of the photon lifetime τ_p ($s\equiv t\tau_p^{-1}$). T and θ are ratios of time constants and were previously defined [$T,\theta=O(10^3)$]. $\Omega_0\equiv\omega_0\tau_p$ is the angular frequency of the solitary laser ω_0 normalized by τ_p^{-1}[$\Omega_0\theta\ (\mathrm{mod}\ 2\pi)=O(1)$]. $\eta\equiv\gamma\tau_p$ is the feedback rate γ normalized by τ_p^{-1}($\eta<1$). P is the excess pump current ($|P|$ is proportional to $J-J_{\mathrm{th}}$ where J and J_{th} are the electrical pump current and its value at the solitary laser threshold, respectively; $|P|<1$). α is the linewidth enhancement factor ($\alpha\sim5-6$).

A basic solution of Eqs. (2) and (3) is a single-frequency solution (constant intensity) of the form

$$Y=A_s\exp[i(\Omega_s-\Omega_0)s]\quad\text{and}\quad Z=Z_s, \tag{4}$$

where A_s, Ω_s, and Z_s are constants. Introducing Eq. (4) into Eqs. (2) and (3), we obtain equations for A_s, Ω_s, and Z_s, which are given in the Appendix. We wish to determine if Eq. (4) admits a Hopf bifurcation to a new solution characterized by time-periodic intensities. To this end, we first rewrite Eq. (2) in terms of the amplitude A and the phase Φ of the complex field defined as

$$Y=A\,\exp[i(\Phi-\Omega_0 s)] \tag{5}$$

and then formulate the linearized equations for $(A,\Phi,Z)=(A_s,\Omega_s s,Z_s)$. The condition for a nontrivial solution of this linearized problem leads to a transcendental characteristic equation for the growth rate λ. Substituting $\lambda=i\omega$ gives two equations for the critical feedback rate η and the frequency ω of the oscillations at the Hopf bifurcation point. They are given by Eqs. (A8) and (A9) in the Appendix.

The simplest approximation of these conditions considers the case $P=O(1)$ and assumes the scaling $\theta=O(T^{1/2})$ and $\eta=O(T^{-1})$ [7]. The leading approximation of the Hopf bifurcation frequency is then the laser relaxation frequency

$$\omega\simeq\sqrt{2PT^{-1}}, \tag{6}$$

which is the well-known result [11]. On the other hand, a Hopf bifurcation may appear at the effective laser threshold (defined by the condition $A_s=0$). The conditions for such a Hopf point are analyzed in the Appendix. We find that the parameter P must be small ($P\sim T^{-1}$) and that the Hopf bifurcation frequency is now inversely proportional to the delay time θ,

$$\omega\simeq\frac{2}{\theta}(\pi+\Delta), \tag{7}$$

where $\Delta\equiv\Omega_s\theta$ is the external cavity mode frequency. Thus, we wish to understand how the Hopf bifurcation frequency ω continuously changes from Eq. (6) to Eq. (7) as $|P|\to0$.

Figure 1 shows the numerically determined Hopf bifurca-

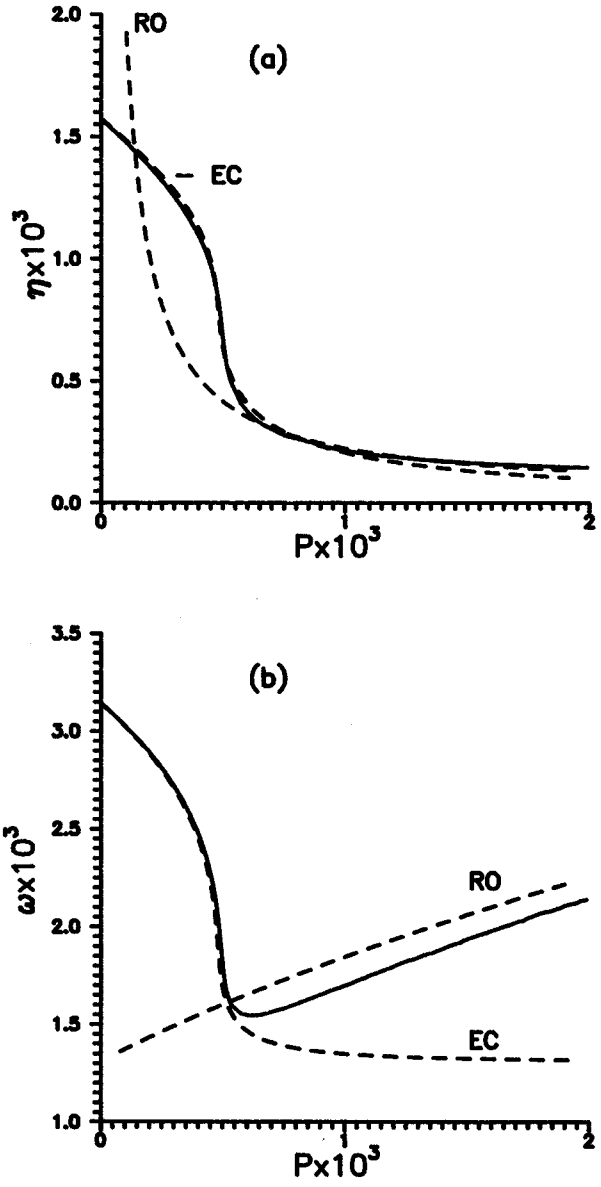

FIG. 1. First Hopf bifurcation. The Hopf bifurcation points have been obtained numerically from the original laser equations (2) and (3) by tracking the critical feedback rate η above which a supercritical transition from steady to time-periodic oscillations is observed, and by evaluating the Hopf conditions (A8) and (A9). The values of the parameters are $\theta=T=1000$, $\alpha=6$, and $\Omega_0\theta(\mathrm{mod}\,2\pi)=-\pi$. The effective laser threshold is exactly located at $P=0$ because $\Omega_0\theta=-\pi$ and $\Delta=-\pi/2$ [see Eq. (A15) and then Eq. (A12)]. We have found numerically that the effect of changing $\Omega_0\theta$ is mainly a shift of the laser threshold to either a positive or a negative P. (a) The dotted line RO represents $\eta=T^{-1}\alpha^{-1}R_H$, where R_H is given by Eq. (18). The dotted line EC represents $\eta=T^{-1}E$ and is obtained from Eqs. (26) and (27). (b) The dotted line RO represents $\omega=T^{-1}\sigma$, where σ is obtained numerically from Eq. (13). The dotted line EC is $\omega=T^{-1}\sigma$, where σ is given by the implicit solution (27).

tion point η and its frequency ω as functions of P. The dotted lines in the figures are approximations that we introduce in Secs. III and IV below. Note that the curves $\eta=\eta(P)$ and $\omega=\omega(P)$ exhibit a layer near $P=0$. As we shall demonstrate, the width of this layer is typically proportional to an $O((T\alpha)^{-1})$ quantity.

In order to determine an approximation of the Hopf bifurcation, we first take into account the fact that $\theta=O(T)$ and $P=O(T^{-1})$ as $T\to\infty$. The leading approximate equations are then examined in terms of α. Specifically, we introduce a small parameter ϵ, defined by

$$\epsilon\equiv T^{-1}, \tag{8}$$

and scale the parameters θ, P, and η and the frequency ω as

$$\theta=\epsilon^{-1}\Theta, \quad P=\epsilon p, \quad \eta=\epsilon E, \text{ and } \omega=\epsilon\sigma. \tag{9}$$

These scalings are satisfied by both Eqs. (6) and (7). After inserting Eq. (9) into the Hopf conditions (A8) and (A9), we find that the unknowns E and σ satisfy Eqs. (A16) and (A17). Unfortunately, the reduced equations are almost identical to the original equations. The idea now is to investigate this problem in terms of α. Because we anticipate a transition layer near the effective laser threshold $p=p_{\rm th}$, our analysis will involve two parts: (1) $p=O(1)$ and $E=O(\alpha^{-1})$ and (2) $p-p_{\rm th}=O(\alpha^{-1})$ and $E=O(1)$. Note that the frequency σ is assumed to be an $O(1)$ quantity for both cases.

III. THE RELAXATION OSCILLATION (RO) FREQUENCY DOMAIN

We examine the domain away from the laser first threshold [i.e., $p=O(1)$ and $p>0$] by seeking a solution of the Hopf conditions (A16) and (A17) of the form

$$E=\alpha^{-1}R \text{ and } \sigma=O(1). \tag{10}$$

We note that $D(\alpha)$, defined by Eq. (A10), simplifies as $D(\alpha)\simeq-\alpha\sin(\Delta)$ and obtain the following equations for R and σ as $\alpha\to\infty$:

$$-2pR\ \sin(\Delta)F_1+\sigma^2=0, \tag{11}$$

$$2p[-R\ \sin(\Delta)F_2-\sigma]+\sigma^3=0. \tag{12}$$

Eliminating R from these two equations and using the definitions of F_1 and F_2, given by Eq. (A18), we find the following equation for σ:

$$\sigma^2-\sigma\ \cot(\sigma\Theta/2)-2p=0. \tag{13}$$

Note that σ is a function of p only.

From Eq. (13), we find that $\sigma=\sigma_c$ at $p=0$, where $0<\sigma_c<\pi/2$ is the root of the equation

$$\sigma_c-\cot(\sigma_c\Theta/2)=0. \tag{14}$$

Furthermore, σ approaches the parabola $\sigma\simeq\sqrt{2p}$ as $p\to\infty$. From Eq. (13), we find a good numerical approximation of $\sigma(p)$ valid for small Θ:

$$\sigma\simeq\sqrt{(2/\Theta)+2p}. \tag{15}$$

The expression (15) clearly shows the competing effects of the laser RO frequency $\sigma=\sqrt{2p}$ and an EC frequency $\sigma=\sqrt{2/\Theta}$.

After determining σ, we find R using Eq. (11). However, Δ in Eq. (11) is a function of R, which satisfies the basic state equation (A1). For α large, Eq. (A1) reduces to the following equation for Δ:

$$\Delta-\Omega_0\theta=-R\Theta\ \cos(\Delta). \tag{16}$$

Using Eqs. (11) and Eq. (16), we eliminate R and obtain an equation for the critical frequency $\Delta=\Delta_H$, at which a Hopf bifurcation occurs. This equation for Δ_H is given by

$$\Delta_H-\Omega_0\theta=\frac{\sigma^2\Theta\ \cot(\Delta_H)}{4p\ \sin^2(\sigma\Theta/2)}. \tag{17}$$

After solving Eq. (17) for Δ_H, we obtain $R=R_H$ from Eq. (11) as

$$R_H=-\frac{\sigma^2}{4p\ \sin(\Delta_H)\sin^2(\sigma\Theta/2)}>0. \tag{18}$$

In Figure 1, the dotted lines RO represent $\eta=T^{-1}E=T^{-1}\alpha^{-1}R_H$ and $\omega=T^{-1}\sigma$ as functions of $P=T^{-1}p$.

Since $p>0$, the condition $R_H>0$ implies the inequality

$$\sin(\Delta_H)<0. \tag{19}$$

The behavior of R_H as a function of p is more difficult to capture analytically. As $p\to0$, $\sigma\to\sigma_c$ and $\cos(\Delta_H)\to0$, from Eq. (17), and $R_H=O(p^{-1})\to\infty$, from Eq. (18). Note that the limit $\cos(\Delta_H)\to0$, together with Eq. (19), implies that

$$\Delta_H(\mathrm{mod}\,2\pi)\to-\pi/2. \tag{20}$$

In Figure 2, we show the bifurcation diagram of the EC mode frequencies Δ as a function of $R\Theta$. The implicit solution $R=R(\Delta)$ is obtained from Eq. (16). Full and broken lines correspond to stable and unstable modes, respectively. The stability conditions are (i) the saddle-node stability condition [12], which reduces to the approximate condition

$$1-R\Theta\ \sin(\Delta)>0 \tag{21}$$

and (ii) the Hopf condition $R<R_H$.

In the next section, we analyze the layer near $p=0$ by introducing a different scaling of the parameters. As $p\to0$, we know that $\sigma\to\sigma_c$, $\Delta_H\ (\mathrm{mod}\,2\pi)\to-\pi/2$, and from Eq. (18) we obtain

$$R_H\to\frac{\sigma_c^2}{4p\ \sin^2(\sigma_c\Theta/2)}. \tag{22}$$

These limits will be the starting point of our analysis near the effective laser threshold.

IV. THE EXTERNAL CAVITY (EC) FREQUENCY DOMAIN

In this section, we investigate the Hopf bifurcation point close to threshold, because our previous approximation fails as p approaches zero [i.e., R_H becomes unbounded as

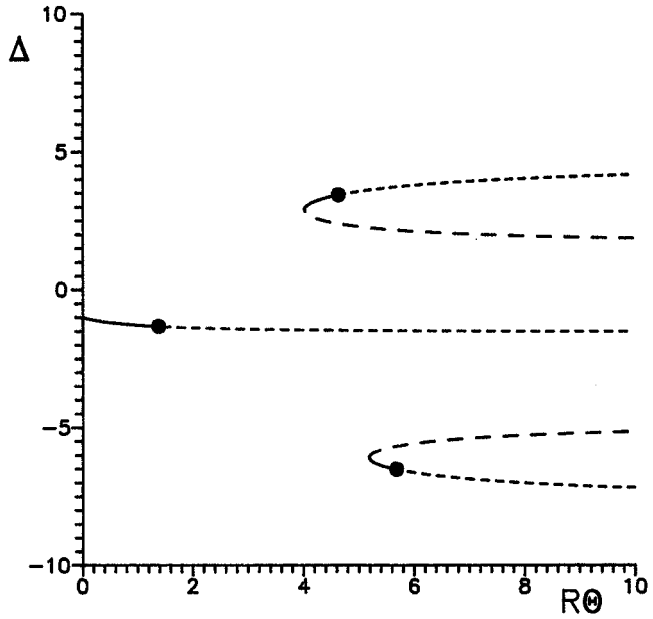

FIG. 2. Bifurcation diagram of the EC frequencies and their bifurcations. Values of the parameters are $\theta=T=1000$, $\alpha=6$, and $\Omega_0\theta(\mathrm{mod}\,2\pi)=-1$, $P=0.001$. The dots correspond to Hopf bifurcation points. The figure represents the EC mode frequency Δ ($\Delta=\Omega_s\theta$) as a function of the scaled feedback rate $R\Theta$ ($R\Theta=\eta\alpha\theta$) and is obtained from Eq. (16). The Hopf bifurcation points are found using Eq. (18).

$p\to 0$, see Eq. (22)]. We resolve this difficulty by assuming the following scaling of the parameters:

$$p=\alpha^{-1}q, \quad E=O(1), \text{ and } \sigma=O(1). \tag{23}$$

Before we determine the leading approximation of the Hopf conditions, it is worthwhile to first inspect the basic state equation (A1). With the scaling (23), we have $\eta\theta=E\Theta=O(1)$ and Eq. (A1) reduces to the condition $\cos(\Delta)=0$ for α large and $\Delta=O(1)$. This is consistent with our previous observation that $\Delta_H(\mathrm{mod}\,2\pi)\to-\pi/2$ near threshold. This implies that the effective laser threshold $p=p_{\mathrm{th}}(E)$ defined by the zero intensity condition [$A_s=0$, or, equivalently, $p_{\mathrm{th}}(E)=-E\cos(\Delta)$] is zero in the first approximation.

Our goal is to find E and σ as functions of p. Equivalently, we may determine E and p as functions of σ. Substituting Eq. (23) into the Hopf conditions (A16) and (A17), assuming $\sin(\Delta)\simeq-1$ and taking the limit α large leads to the following equations for E and σ:

$$2qEF_1-[E^2(F_1^2-F_2^2)-\sigma^2]+2\sigma E^2F_1F_2=0, \tag{24}$$

$$2qEF_2-2E^2F_1F_2-\sigma[E^2(F_1^2-F_2^2)-\sigma^2]=0. \tag{25}$$

Eliminating q, we obtain a quadratic equation for $E(\sigma)$:

$$E^2(F_2+\sigma F_1)+\sigma^2\,\frac{F_2-\sigma F_1}{F_1^2+F_2^2}=0. \tag{26}$$

Using Eq. (25), we find q and then p:

$$q\equiv\alpha p=-\frac{1}{2EF_2}\{-2E^2F_1F_2-\sigma[E^2(F_1^2-F_2^2)-\sigma^2]\}. \tag{27}$$

The dotted lines EC in Fig. 1 represent $\eta=T^{-1}E$ and $\omega=T^{-1}\sigma$ in terms of $P=T^{-1}p$.

As q increases, E decreases, and from Eq. (26) we find the limit $F_2=\sigma F_1$, which implies $\sigma\to\sigma_c$. Using Eq. (27), we then obtain

$$q=\alpha p\to\frac{\sigma_c^2}{4E\,\sin^2(\sigma_0\Theta/2)}, \tag{28}$$

which matches Eq. (22) if $E=\alpha^{-1}R$. Thus, we have shown that our two approximations overlap.

Finally, we may determine the leading approximation of the Hopf bifurcation point and its frequency at the threshold. In the first approximation for α large, $p_{\mathrm{th}}=0$ and the conditions (24) and (25) are satisfied if $F_2=0$ and $E^2F_1^2-\sigma^2=0$, or, equivalently, if

$$\sigma=\frac{n\pi}{\Theta} \text{ and } E=\frac{\sigma}{2} \quad (n=1,3,\ldots). \tag{29}$$

Equation (29) clearly displays a frequency that is only controlled by the delay of the feedback.

V. SUMMARY

In this section, we summarize our main results. The bifurcation point is characterized by a critical value of the feedback rate η and by the frequency ω of the oscillations at that point. Depending on the scaling of P, we have found two different limits.

(1) The RO domain [$P=O(T^{-1})$] appears for low values of P and is characterized by a frequency that is close to the frequency of the relaxation oscillations of the solitary laser:

$$\omega\simeq\sqrt{(2/T)[(1/\theta)+P]}. \tag{30}$$

In Eq. (30), we note the progressively stronger effect of the delay θ as P decreases. The critical value of the feedback rate is given by

$$\eta\simeq-\frac{\omega^2}{4P\alpha\,\sin(\Delta_H)\sin^2(\omega\theta/2)}>0, \tag{31}$$

where Δ_H satisfies the transcendental equation (17). This expression is equivalent to the approximation of the bifurcation point for moderate values of the pump [7]. Thus, it is the frequency of the oscillations that first changes as the pump parameter is decreased.

(2) The EC domain [$P=O(T^{-1}\alpha^{-1})$] appears for very low values of the pump and is characterized by a dominant effect of the external cavity. The expressions are of the form $\omega=T^{-1}\sigma$ and $\eta=T^{-1}E$, where σ and E are given, in parametric form, by Eqs. (26) and (27). Near threshold,

$$\omega\simeq\frac{\pi}{\theta} \text{ and } \eta\simeq\frac{\omega}{2}, \tag{32}$$

which clearly exhibits the dominant effect of the delay θ.

VI. DISCUSSION

The bifurcation to time-periodic intensity regimes for a semiconductor laser subject to optical injection is studied using Lang and Kobayashi equations. We concentrated on low values of the pump parameter P and derive two distinct asymptotic approximations of the Hopf bifurcation point. Our approximations are in good agreement with the numerical estimates of the Hopf bifurcation point and its frequency (see Fig. 1). The numerical location of the Hopf bifurcation point has been obtained by numerically integrating Eqs. (2) and (3) and looking for the onset of time-dependent intensities. It has also been obtained by direct evaluation of the Hopf conditions using the complete characteristic equation.

The approximation (1) formulated by Tatah and Garmire [5] and Sacher, Elsasser, and Gobel [6] corresponds to the first regime [i.e., $P=O(T^{-1})$]. This can be shown by evaluating Eq. (12) for small Θ and with $\sin(\Delta)=-1$. We find

$$\sigma=\left(\frac{2p}{1+R\Theta}\right)^{1/2}, \tag{33}$$

which is Eq. (1) rewritten in terms of our new variables. We conclude that the approximation (1) is valid provided that the delay θ is not too large, that the EC mode frequency Δ is close to $-\pi/2$, and that the pump parameter P is not too small. For larger θ, the frequency $\omega=\omega(P)$ can be obtained by solving Eq. (13) implicitly. Note from Eq. (13) that the frequency does not depend on Δ. However, this is no more the case if P is very small, close to the threshold. Then the solution is obtained in parametric form from Eqs. (26) and (27).

The specific scaling that characterizes each domain in P is useful if we examine the nonlinear problem [10]. In the RO domain, the proper time scale is $S=\omega s$ (ω is the RO frequency) and the feedback rate is very low [$\eta=O(T^{-1}\alpha^{-1})$]. Using this information, it can be shown that the nonlinear problem reduces to the *linearized* solitary laser equations coupled nonlinearly to the phase of the laser field [13]. This explains the numerical observation of nearly harmonic intensity oscillations exhibiting a frequency close to the RO frequency of the solitary laser. However, this is no longer the case in the EC domain. In this domain, the frequency strongly depends on the delay θ and the feedback rate is larger [$\eta=O(T^{-1})$]. Using the scalings appropriate for the EC domain, we have found that the approximation of the nonlinear problem exhibits a stronger amplitude-phase coupling [13]. This leads to pulsating intensity oscillations which need to be investigated in detail.

ACKNOWLEDGMENTS

This research was supported by U.S. Air Force Office of Scientific Research Grant No. AFOSR F49620-95-0065, National Science Foundation Grant No. DMS-9625843, NATO Collaborative Research Grant No. 961113, the Fonds National de la Recherche Scientifique (Belgium), and the Inter-University Attraction Pole of the Belgian government.

APPENDIX: THE SINGLE MODE SOLUTION AND THE HOPF BIFURCATION CONDITIONS

A basic reference solution of LK equations (2) and (3) is the single frequency solution (4). Introducing Eq. (4) into Eqs. (2) and (3) leads to three equations for the constants A_s, Ω_s, and Z_s, given by

$$\Delta-\Omega_0\theta=-\eta\theta[\alpha\cos(\Delta)+\sin(\Delta)], \tag{A1}$$

$$A_s^2=\frac{P+\eta\cos(\Delta)}{1-2\eta\cos(\Delta)}\geqslant 0, \tag{A2}$$

$$Z_s=-\eta\cos(\Delta), \tag{A3}$$

where Δ is the EC mode frequency defined by

$$\Delta\equiv\Omega_s\theta. \tag{A4}$$

As η progressively increases from zero, the number of possible solutions increases but always remains odd. Note that the inequality in Eq. (A2) implies the condition

$$P\geqslant-\eta\cos(\Delta) \tag{A5}$$

if η is small.

We wish to determine the conditions for a Hopf bifurcation from the single frequency solution (4). To this end, we rewrite Eq. (2) in terms of the amplitude A and the phase Φ, defined by $Y=A\exp[i(\Phi-\Omega_0 s)]$. From the linearized equations for $(A,\Phi,Z)=(A_s,\Omega_s s,Z_s)$, we determine the condition for a nontrivial solution which then leads to a transcendental equation for the growth rate λ. Using Eq. (A2), we eliminate A_s from its coefficients and obtain

$$2\epsilon(P-Z)[-(ZF+\lambda)-\eta\sin(\Delta)F\alpha]-\left[\epsilon\frac{1+2P}{1+2Z}+\lambda\right]\times[\eta^2F^2-2\lambda\eta\cos(\Delta)F+\lambda^2]=0, \tag{A6}$$

where F is defined by

$$F\equiv\exp(-\lambda\theta)-1. \tag{A7}$$

In Eq. (A6), we have omitted the subscripts s for Z [Z now means Eq. (A3)]. The small parameter ϵ is defined by expression (8). The conditions for a Hopf bifurcation are obtained by substituting $\lambda=i\omega$ into Eq. (A6) and by separating the real and imaginary parts. We find two conditions for the critical feedback rate η and the frequency ω:

$$2\epsilon[P+\eta\cos(\Delta)]\eta F_1D-\epsilon\frac{1+2P}{1-2\eta\cos(\Delta)}[\eta^2(F_1^2-F_2^2)+2\omega\eta\cos(\Delta)F_2-\omega^2]+2\omega\eta F_1[\eta F_2-\omega\cos(\Delta)]=0, \tag{A8}$$

$$2\epsilon[P+\eta\cos(\Delta)][\eta F_2D-\omega]-\epsilon\frac{1+2P}{1-2\eta\cos(\Delta)}2\eta F_1[\eta F_2-\omega\cos(\Delta)]-\omega[\eta^2(F_1^2-F_2^2)+2\omega\eta\cos(\Delta)F_2-\omega^2]=0, \tag{A9}$$

where

$$D \equiv \cos(\Delta) - \sin(\Delta)\alpha \tag{A10}$$

and

$$F_1 \equiv \cos(\omega\theta) - 1 \quad \text{and} \quad F_2 \equiv -\sin(\omega\theta). \tag{A11}$$

We next examine the particular case of a Hopf bifurcation at the laser first threshold.

1. Hopf bifurcation at the laser first threshold

At the laser first threshold, the laser intensity is zero. From Eq. (A2), this implies the condition

$$P + \eta\ \cos(\Delta) = 0. \tag{A12}$$

Inserting $\lambda = i\omega$ into Eq. (A6), and using the fact that $P - Z = 0$ from Eq. (A12), we obtain the condition

$$\eta^2 F^2 - 2i\omega\eta\ \cos(\Delta) F - \omega^2 = 0, \tag{A13}$$

where $F = F_1 - iF_2$ and F_1, F_2 are defined by Eq. (A11). From the real and imaginary parts of Eq. (A13), we find the following solution if $\Delta < 0$ (we obtain similar conditions if $\Delta > 0$):

$$\eta = -\frac{\pi + \Delta}{\theta\ \sin(\Delta)} > 0 \quad \text{and} \quad \omega = \frac{2}{\theta}(\pi + \Delta). \tag{A14}$$

In Eq. (A14), Δ satisfies Eq. (A1) or, equivalently, using Eq. (A14),

$$\Omega_0\theta + \pi + \alpha(\pi + \Delta)\cot(\Delta) = 0. \tag{A15}$$

2. Hopf bifurcation conditions for low pump

We are interested in solving the Hopf bifurcation conditions assuming $\theta = O(T)$ and $P = O(T^{-1})$. We introduce the expressions (9) for θ, P, η, and ω into Eqs. (A8) and (A9) and take the limit $\epsilon \to 0$. The leading order equations are $O(\epsilon^3)$ and are given by

$$2[p + E\ \cos(\Delta)]EF_1 D - [E^2(F_1^2 - F_2^2) + 2\sigma E\ \cos(\Delta)F_2 - \sigma^2] + 2\sigma E F_1[EF_2 - \sigma\ \cos(\Delta)] = 0, \tag{A16}$$

$$2[p + E\ \cos(\Delta)][EF_2 D - \sigma] - 2EF_1[EF_2 - \sigma\ \cos(\Delta)] - \sigma[E^2(F_1^2 - F_2^2) + 2\sigma E\ \cos(\Delta)F_2 - \sigma^2] = 0, \tag{A17}$$

where F_1 and F_2 defined by Eq. (A11) are rewritten in terms of $\sigma\Theta$ as

$$F_1 \equiv \cos(\sigma\Theta) - 1 \quad \text{and} \quad F_2 \equiv -\sin(\sigma\Theta). \tag{A18}$$

These equations are analyzed for α large in Secs. III and IV.

[1] I. Fisher, G. H. M. van Tartwijk, A. M. Levine, W. Elsässer, E. Göbel, and D. Lenstra, Phys. Rev. Lett. **76**, 220 (1996).

[2] T. Sano, Phys. Rev. A **50**, 2719 (1994).

[3] G. H. M. van Tartwijk, A. M. Levine, and D. Lenstra, IEEE J. Sel. Top. Quantum Electron. **1**, 466 (1995).

[4] M. Fujiwara, K. Kubato, and R. Lang, Appl. Phys. Lett. **38**, 217 (1981).

[5] K. Tatah and E. Garmire, IEEE J. Quantum Electron. **25**, 1800 (1989).

[6] J. Sacher, W. Elsasser, and E. O. Gobel, IEEE J. Quantum Electron. **27**, 373 (1991).

[7] T. Erneux, G. H. M. van Tartwijk, D. Lenstra, and A. M. Levine, SPIE **2399**, 170 (1995).

[8] A. M. Levine, G. H. M. van Tartwijk, D. Lenstra, and T. Erneux, Phys. Rev. A **52**, R3436 (1995).

[9] R. Lang and K. Kobayashi, IEEE J. Quantum Electron. **QE-16**, 347 (1980).

[10] P. M. Alsing, V. Kovanis, A. Gavrielides, and T. Erneux, Phys. Rev. A **53**, 4429 (1996).

[11] A. Ritter and H. Haug, J. Opt. Soc. Am. B **10**, 130 (1993); **10**, 145 (1993).

[12] D. Lenstra, M. van Vaalen, and B. Jaskorzynska, Physica **125C**, 225 (1984).

[13] T. Erneux, P. M. Alsing, V. Kovanis, and A. Gavrielides, SPIE **2693**, 701 (1996).